BIOCHEMISTRY
including biophysical chemistry & molecular biology

Article

pubs.acs.org/biochemistry

Toward Understanding the Mechanism of Ion Transport Activity of Neuronal Uncoupling Proteins UCP2, UCP4, and UCP5

Tuan Hoang,[†,‡] Matthew D. Smith,[‡,§] and Masoud Jelokhani-Niaraki*[,†,‡]

[†]Department of Chemistry, Wilfrid Laurier University, Waterloo, ON, Canada

[‡]Biophysics Interdepartmental Group, University of Guelph, Guelph, ON, Canada

[§]Department of Biology, Wilfrid Laurier University, Waterloo, ON, Canada

Supporting Information

ABSTRACT: Neuronal uncoupling proteins (UCP2, UCP4, and UCP5) have crucial roles in the function and protection of the central nervous system (CNS). Extensive biochemical studies of UCP2 have provided ample evidence of its participation in proton and anion transport. To date, functional studies of UCP4 and UCP5 are scarce. In this study, we show for the first time that, despite a low level of amino acid sequence identity with the previously characterized UCPs (UCP1−UCP3), UCP4 and UCP5 share their functional properties. Recombinantly expressed in *Escherichia coli*, UCP2, UCP4, and UCP5 were isolated and reconstituted into liposome systems, where their conformations and ion (proton and chloride) transport properties were examined. All three neuronal UCPs are able to transport protons across lipid membranes with characteristics similar to those of the archetypal protein UCP1, which is activated by fatty acids and inhibited by purine nucleotides. Neuronal UCPs also exhibit transmembrane chloride transport activity. Circular dichroism spectroscopy shows that these three transporters exist in different conformations. In addition, their structures and functions are differentially modulated by the mitochondrial lipid cardiolipin. In total, this study supports the existence of general conformational and ion transport features in neuronal UCPs. On the other hand, it also emphasizes the subtle structural and functional differences between UCPs that could distinguish their physiological roles. Differentiation between structure−function relationships of neuronal UCPs is essential for understanding their physiological functions in the CNS.

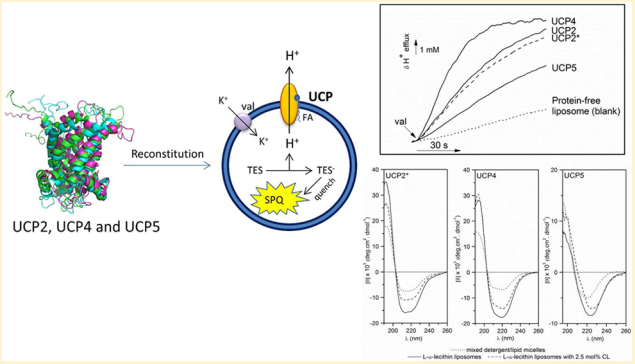

Uncoupling proteins (UCPs), located in the inner membrane of mitochondria, uncouple oxidative phosphorylation from ATP synthesis by dissipating the proton gradient across the inner membrane.[1] Five human UCP homologues have been identified in different tissues to date; UCP1 is the only member of the UCP family with a well-characterized thermogenic role in brown adipose tissue.[2] UCP1-mediated proton leak, which causes uncoupling effects, is known to be activated by fatty acids (FAs) and inhibited by purine nucleotides.[1,2] The structure of UCP1 is proposed to consist of three repeated domains (tripartite structure), each of which is comprised of two hydrophobic transmembrane α-helical regions spanning the inner mitochondrial membrane.[1] With no high-resolution structure available, the structures of the prototypical UCP1 and other UCPs have been assumed to resemble the crystal structure of the ADP/ATP carrier (AAC).[1] Recently, a structural study of UCP2 by NMR molecular fragment searching revealed striking similarities between UCP2 and AAC.[3]

Three of the five human UCP homologues, namely, UCP2, UCP4, and UCP5, are located in the central nervous system (CNS) and are therefore believed to serve unique roles in neurons.[4] These roles could be directly related to many neurodegenerative diseases, including epilepsy, Parkinson's disease, Alzheimer's disease, ischemia/stroke, brain injury, and aging.[4] A high level of amino acid sequence identity to UCP1 (59%) and ubiquitous expression have made UCP2 an attractive target for many recent studies.[1,2,4] These studies have mostly focused on UCP2 and its ability to suppress the production of reactive oxygen species (ROS) in mitochondria.[1,2,4] This function of UCP2 could represent a protective mechanism against oxidative stress in various tissues (liver, endothelium, and neurons). On the other hand, UCP2 expressed in pancreatic β-cells has been proposed to be a negative regulator for glucose-induced insulin secretion, which is linked to type 2 diabetes.[4] Despite inconsistencies between different studies, the regulation of proton transport in UCP2 and its mechanism(s) of activation and inhibition have generally been confirmed to be similar to those of UCP1.[5,6]

Although both UCP4 and UCP5 [also called brain mitochondrial carrier protein-1 (BMCP1)] are more widespread in the brain than UCP2, little is known about these two

Received: February 6, 2012
Revised: April 20, 2012
Published: April 23, 2012

ACS Publications © 2012 American Chemical Society

proteins.[2] They have low levels of amino acid sequence identity with the prototypical protein UCP1 (34% for UCP4 and 30% for UCP5); on the other hand, UCP4 and UCP5 share many of the amino acids that are considered characteristic features of the UCP family and are predicted to have the same overall membrane topology.[7] Despite the similarities, it is still debated whether UCP4 and UCP5 belong to the UCP family.[1,2,4] UCP4 was originally found to be expressed in the brain,[8] but its expression has also recently been detected in adipocytes.[9] UCP5, on the other hand, is expressed in diverse tissues and organs, including brain (cortex, hypothalamus, limbic system, cerebellum, basal ganglia, and spinal cords), testis, uterus, kidney, lung, stomach, liver, and heart.[2,4,10] There is also evidence of the presence of mRNA for UCP5 isoforms in fruit flies, supporting an important and evolutionarily retained function of this putative UCP in the CNS.[11] Moreover, three isoforms of UCP5 have been found in humans, suggesting a level of complexity in the regulatory function of UCP5 in the brain.[2,12] UCP4 has also been reported to have isoforms of varying lengths.[13] The significance of UCP4 and UCP5 in cell metabolism and survival has been confirmed in many cell culture studies.[14−17] However, because of their low level of sequence identity with other UCPs and current lack of evidence of proton transport activity, the question of whether UCP4 and UCP5 are genuine mitochondrial UCPs remains to be answered.[1,2,4]

Being a major lipid component of the inner mitochondrial membrane, cardiolipin (CL) has been shown in many studies to strongly impact the structure and function of mitochondrial carrier proteins.[18−23] Acting as a "double phospholipid", CL has two phosphatidylglycerols connected through a glycerol backbone in the center to form a unique dimeric structure. The crystal structure of AAC, the main structural model for UCPs, was observed to be bound to three CL molecules; this interaction was suggested to promote protein association.[18] With CL located in the inner mitochondrial membrane, it would not be surprising that UCPs also interact with CL. However, the effect of CL on the structure and function of UCPs has not been investigated in detail.

Our previous study demonstrated that neuronal UCP4 and UCP5 share common conformational and ligand binding properties with UCP1−UCP3.[24] In this study, we show for the first time that neuronal UCP4 and UCP5 reconstituted into liposomes also exhibit proton and chloride transport activities comparable to those of other UCPs. In addition, the effect of CL on the conformation and function of UCP2, UCP4, and UCP5 is investigated in some detail. In total, this study provides evidence that UCP4 and UCP5 should be considered as genuine components of the UCP family of proteins.

EXPERIMENTAL PROCEDURES

UCP Constructs and Chemicals. The human UCP2 cDNA clone (pET-UCP2) was a gift from M. Brand (MRC Dunn Human Nutrition Unit, Cambridge, U.K.). Neuronal His-tagged UCP constructs were cloned into the pET21d expression vector and transformed into *Escherichia coli* BL21(DE3) [with the exception of UCP4, which was introduced into *E. coli* BL21 CodonPlus (DE3)] for expression, as described previously.[24] Under our experimental conditions, the conformation and ion transport function of UCP2 with and without a His tag were similar[24,25] (Figures 1 and 2A); consequently, the highly pure non-His-tagged UCP2 (shown as UCP2* in all figures and tables in the Supporting Information) was used in all conformational and functional experiments. His-tagged versions of UCP4 and UCP5 (shown as UCP4 and UCP5, respectively, in all figures) were used for all experiments. Egg yolk L-α-lecithin (Sigma, St. Louis, MO) contained at least 60% (by weight) phosphatidylcholine. The remaining 40% was comprised mostly of phosphatidylethanolamine and other lipids. CL [1′,3′-bis(1,2-dioleoyl-*sn*-glycero-3-phospho)-*sn*-glycerol (sodium salt)] and the detergent C_8E_4 (octyltetraoxyethylene) were obtained from Avanti Polar Lipids (Alabaster, AL) and Bachem (Torrance, CA), respectively. Triton X-100 (TX-100), Triton X-114 (TX-114), and sarcosyl (*N*-lauroylsarcosine, sodium salt) were from Calbiochem-EMD Biosciences (Gibbstown, NJ). The fluorescent probe 6-methoxy-*N*-(3-sulfopropyl)quinolinium (SPQ) (99%) was from Biotium Inc. (Burlington, ON). All other chemicals were purchased from Sigma.

Expression, Extraction, and Reconstitution of UCPs. All recombinant neuronal UCPs were overexpressed in *E. coli* from cloned versions of the cDNAs using 1 mM isopropyl β-D-thiogalactoside (IPTG) as described previously.[24] Recombinant UCPs were extracted as described previously,[5] with some modifications. Inclusion bodies were washed stepwise with 2% (w/v) TX-100, 2% (w/v) TX-114, and 0.1% (w/v) sarcosyl in extraction buffer [20 mM Tris-HCl and 500 mM NaCl (pH 8.0)]. The final pellet fraction was resuspended in 4 mL of buffer A [50 mM CAPS, 25 mM DTT, 2 mM PMSF, and 10% glycerol (pH 10.0)] and 2% (w/v) sarcosyl. This mixture was incubated for 45 min at room temperature followed by 15 min at 4 °C. Insoluble proteins were removed by centrifugation (14000*g* for 10 min). The supernatant was diluted with 6 mL of buffer B (10% glycerol and 1% TX-114), supplemented with 1 mM ATP. After a 2 h incubation at 4 °C, the mixture was dialyzed three times against 300 mL (4:6 buffer A:buffer B ratio) to remove sarcosyl. The final dialyzed protein was supplemented with 5 mg/mL L-α-lecithin and 1 mM ATP, incubated for 2 h at 4 °C, and concentrated ∼2-fold in an Ultrafree-15 centrifugal filter device (Millipore). Protein purity and concentration were analyzed using sodium dodecyl sulfate−polyacrylamide gel electrophoresis (SDS−PAGE) and a Lowry-based protein assay (Bio-Rad, Hercules, CA),[26] respectively.

In both CD spectroscopic and ion transport experiments, extracted UCPs were reconstituted into liposomes using a detergent-mediated reconstitution method.[5,6] Two phospholipid systems were used in this study, L-α-lecithin with and without 2.5 mol % CL. Briefly, lipids were dissolved in chloroform, dried overnight under vacuum, and rehydrated in the desired buffer. For CD measurements, 10 mM potassium phosphate buffer (pH 7.2) was used. For ion transport experiments, the internal buffer containing the fluorescent probe SPQ was used at pH 7.2. Phospholipids were solubilized with C_8E_4 to a final detergent:phospholipid ratio of 2.5 by mass. Extracted proteins were then added to the mixed lipid/detergent micelles in each particular experiment. In CD conformational studies, the final protein:lipid molar ratio was ∼1:1000. In ion transport experiments, this ratio was 1:10000 (equivalent to a 1:250 protein:lipid weight ratio). Protein-free liposome controls were prepared in parallel for all experiments. SM-2 Biobeads (Bio-Rad) were used to remove detergents for liposomes to form spontaneously. In ion transport assays, the external SPQ probe was removed using a coarse Sephadex G25-300 (GE Healthcare) spin column.

Liposome Size Measurements. The size and homogeneity of liposomes and proteoliposomes were determined by dynamic light scattering (DLS) using a Zetasizer Nano ZS (Malvern Instruments, Worcestershire, U.K.). The results reported are the average of 5−10 measurements.

CD Spectroscopic Measurements. Far-UV CD spectra were recorded on an Aviv 215 spectropolarimeter (Aviv Biomedical). Ellipticities are reported as mean residue ellipticity. All far-UV CD measurements were taken in 0.1 cm path length quartz cells at 0.5 nm resolution (25 °C). The reported spectra were an average of eight scans. The secondary structure content of proteins was estimated from CD spectra using the deconvolution program CDSSTR, and the analysis was based on a set of 48 reference proteins and performed on the Dichroweb website.[27,28]

Fluorescence Measurements. Steady-state fluorescence measurements were taken in a Cary Eclipse spectrophotometer (Varian). The excitation bandwidth slit for all measurements was 5 nm, and a scan speed of 600 nm/min was used throughout the experiments (25 °C).

Proton and Chloride Transport Measurements. Ion transport mediated by reconstituted UCPs across the lipid membranes was measured by the anion-sensitive fluorescence quenching method. The SPQ fluorescent dye was chosen for this study because of its ability to measure both anion (chloride, bromide, and iodide) and proton transport.[29] During chloride transport measurements, the fluorescence of SPQ (λ_{ex} = 347 nm; λ_{em} = 442 nm) was quenched directly by the chloride anions. On the other hand, proton transport is measured indirectly through the quenching of SPQ fluorescence by *N*-[tris(hydroxymethyl)methyl]-2-aminoethanesulfonic acid anion (TES^-). In a low-pH environment (pK_a of TES of ∼7.4), TES is fully protonated and does not affect SPQ's fluorescence. Upon the loss of a proton (at high pH), the TES anion collisionally quenches SPQ's fluorescence.

In each transport assay, 40 μL of proteoliposomes (∼0.8 mg of lipid) was incubated with 1.96 mL of external medium. Osmotic pressure was kept balanced across the lipid membrane. In the proton transport assay, the internal medium consisted of TES buffer (30 mM), TEA_2SO_4 (80 mM), and EDTA (1 mM). The external buffer in this case contained K_2SO_4 (80 mM) instead of TEA_2SO_4. In the chloride transport assay, the internal medium consisted of 10 mM sodium phosphate, 133 mM TEA_2SO_4, and 1 mM EDTA and the external medium contained 10 mM sodium phosphate, 200 mM KCl, and 1 mM EDTA. All transport assay buffers were kept at pH 7.2. Ion transport in each experiment was driven by the influx of K^+ from the external buffer mediated by the K^+ ionophore valinomycin (val). Upon the inward diffusion of K^+ across the membrane, the osmotic balance was disrupted and functional UCPs transported protons (out) or chlorides (in) to offset this discrepancy in membrane potential. Lauric acid (LA) was added to activate proton transport. All ion transport data were corrected by subtraction from the nonspecific proton leak and calibrated for the SPQ fluorescence response and internal volume of proteoliposomes.[29] Briefly, the internal volume of the vesicles for each preparation was calculated from the volume of the distribution of the fluorescent probe SPQ. To measure this, the fluorescent SPQ trapped in liposome was released using a small amount of detergent. The concentration of trapped SPQ was measured by the standard addition method, by sequential addition of SPQ with a known concentration into the mixture. Plotting of the SPQ fluorescence signal versus $[SPQ]_{added}$ yielded the original concentration of SPQ trapped in the liposomes. This information is used to calculate the internal volume of the liposome. In addition, liposome sizes were measured using the dynamic light scattering technique, which confirmed a monodisperse population with radii varying from 60 to 100 nm.

The final protein content in proteoliposomes was calculated using the modified Lowry concentration assay. Phospholipids, which interfere with the Lowry assay, were removed from the proteoliposomes after trichloroacetic acid (TCA) precipitation. Briefly, 100−150 μL proteoliposome samples or bovine serum albumin (BSA) standards were precipitated with trichloroacetic acid (TCA) and redissolved in 25 μL of SDS. Developing reagents [reagents A and B (Bio-Rad)] were added to each fraction. The mixtures were incubated for 15 min at room temperature, and absorbance was measured at 750 nm.

Amino Acid Sequence Analysis and Structural Modeling of Neuronal UCPs. Protein sequence analysis and primary sequence alignment of UCPs and AAC were performed using T-Coffee.[30,31] All three-dimensional structural models of UCPs were obtained using MODELER 9.9[32] after the sequence alignment based on the crystal structures of AAC reported in 2005 (Protein Data Bank entry 2C3E).[18] The three CLs associated with AAC in the crystal structure were superimposed in the UCP models for analysis. Structural models were viewed using Pymol.[33]

Statistical Analysis. Data were analyzed using the one-way analysis of variance (ANOVA) statistical method. A p of <0.05 was considered statistically significant.

RESULTS

Expression of UCPs and Their Reconstitution into Liposomes. Recombinant UCPs extracted from purified inclusion bodies were confirmed to have high purity using SDS−PAGE before being reconstituted into liposomes (Figure 1). Dynamic light scattering (DLS) measurements confirmed the presence of monodisperse proteoliposome populations for all reconstituted UCP samples. The sizes of blank L-α-lecithin and protein-reconstituted vesicles were in the range of large unilamellar vesicles (LUVs) (60−100 nm radii) (Table S1 of the Supporting Information). Addition of CL (2.5 mol %) into the phospholipid system slightly enlarged the size of the liposomes (Table S1 of the Supporting Information). Reconstitution of UCPs into the liposomes at a low protein:lipid ratio, used in the transport assays, did not significantly change the size of the liposomes except for those with UCP4. The size of UCP4 proteoliposomes decreased in the CL-free lipid system but increased in the CL-containing lipid system, compared to the blank liposomes (Table S1 of the Supporting Information).

UCP-Mediated Proton Transport. Proton transport mediated by reconstituted neuronal UCPs was measured in two phospholipid systems, L-α-lecithin vesicles with and without 2.5 mol % CL. As shown in Figure 2A, all reconstituted neuronal UCPs conducted protons across the phospholipid bilayer in the presence of fatty acid activator LA. All measurements showed that efflux of protons occurred within 15−20 s of the addition of the K^+ ionophore val to initiate ion transport. The measured UCP-mediated transport rates were subtracted from the nonspecific proton leak (from protein-free blank liposomes) and corrected for the final protein content in proteoliposomes. It is also important to note that the presence of reconstituted UCPs in liposome did not produce any

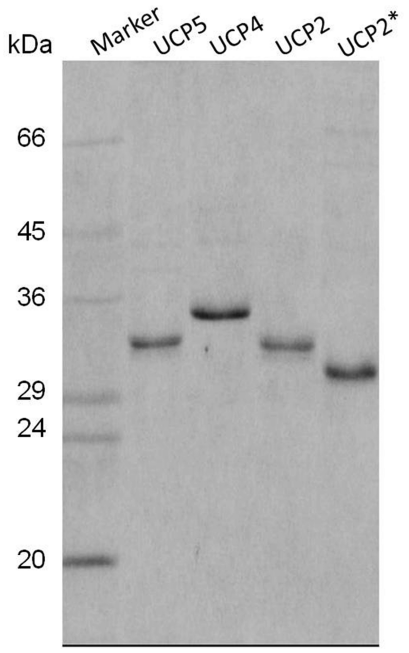

Figure 1. Expression and purification of recombinant human neuronal UCPs. The proteins were expressed in *E. coli* in the inclusion body fraction. Inclusion bodies were extracted and purified as described in Experimental Procedures. The proteins were obtained in high purity and resolved using SDS−PAGE (12% gel) and stained with Coomassie Brilliant Blue. The molecular mass (kilodaltons) markers are indicated at the left. UCP2 was expressed in its His-tagged (UCP2) and non-His-tagged (UCP2*) forms. UCP4 and UCP5 were expressed only in their His-tagged forms.

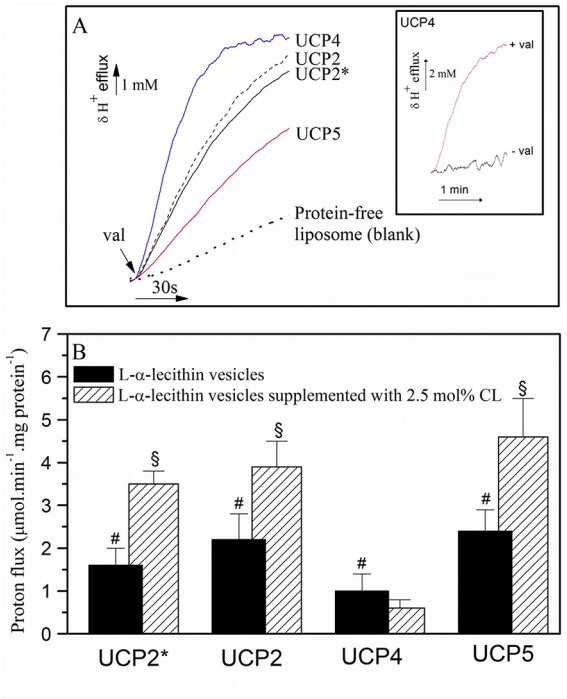

Figure 2. Transport of protons mediated by neuronal UCPs across the phospholipid vesicles. (A) Recorded H^+ efflux through phospholipid vesicles reconstituted with neuronal UCPs. Proton transport was activated by addition of 100 μM LA. Valinomycin (val) was added at a concentration of 1 μM to initiate proton transport. A protein-free liposome blank displays nonspecific proton leak. The inset shows that no significant nonspecific leakage of the reconstituted UCP4 (or other neuronal UCPs) into the liposome was observed (−val); the leakage is due primarily to the transport of protons across the membrane mediated by UCPs (+val). This result holds for UCP2 and UCP5, as well. (B) Average corrected proton transport rate mediated by neuronal UCPs in two phospholipid systems, L-α-lecithin with and without 2.5 mol % CL. Results are presented as the initial H^+ transport that was already subtracted from the nonspecific proton leak and corrected for the internal liposomal volume and protein content in the proteoliposomes. The rates are the means of 15−20 independent measurements ± the standard error of the mean. In L-α-lecithin vesicles, proton transport rates of UCP2*, UCP2, UCP4, and UCP5 are 1.6 ± 0.4, 2.2 ± 0.6, 1 ± 0.4, and 2.4 ± 0.5 μmol min^{-1} (mg of protein)$^{-1}$, respectively. In L-α-lecithin vesicles with 2.5 mol % CL, these rates are 3.5 ± 0.3, 3.9 ± 0.6, 0.6 ± 0.2, and 4.6 ± 0.9 μmol min^{-1} (mg of protein)$^{-1}$, respectively. The phospholipid concentration was 20 mg/mL; the final protein content in the liposomes was 2−5 μg/mg of lipid. The final proton transport rates were calculated in the presence of 100 μM LA and on the basis of the total protein concentration present in the liposomes; the orientations of the reconstituted proteins were ignored in this calculation. UCP2* is the non-His-tagged version of human UCP2. All other UCPs are in their His-tagged forms. A one-way ANOVA statistical test was performed to determine the statistical significance of data, and p values were obtained. $p < 0.05$ when comparing the proton transport mediated by UCPs to the basal proton leakage (#), and $p < 0.05$ when comparing the proton transport mediated by UCPs in the CL-supplemented vesicles to that in L-α-lecithin vesicles (§).

nonspecific leakage (inset of Figure 2A). In addition, spectroscopic analysis confirms that no traces of detergent are present after reconstitution that otherwise could cause leakage across the vesicle membrane (Figure S1 of the Supporting Information). Thus, the proton transport reported in this study is UCP-specific. The final corrected proton flux for all reconstituted neuronal UCPs is shown in Figure 2B. Overall, all neuronal UCPs displayed comparable transport rates in L-α-lecithin vesicles [1−2 μmol min^{-1} (mg of protein)$^{-1}$]. The proton fluxes for UCP2 and its His-tagged version (Figure 2B) were also very similar, which reconfirms the conformational equivalence of the two forms of the protein.[25] Addition of CL to the phospholipid vesicles at 2.5 mol % induced changes in the proton transport rate of all neuronal UCPs (Figure 2B). In this vesicle system, the rate of proton transport mediated by UCP2 and UCP5 was approximately doubled, whereas UCP4-mediated proton flux decreased slightly (Figure 2B). It should be noted that the proton flux rates were calculated on the basis of the total protein content of the liposomes and proteins' orientation across the membranes were not considered in these calculations. Considering the orientation of the reconstituted proteins can increase the overall transport rate (decrease in protein effective concentration), on the basis of our experimental results, approximately 50% of the proteins are oriented in the correct direction for proton transport and transport rates can therefore increase up to 2 times (see the section on the inhibition of UCP-mediated proton flux). The proton transport rates reported in this study are in the range of the previously published data for reconstituted UCP1−UCP3 (Table S3 of the Supporting Information). In all previous experiments (regardless of the reconstitution system and experimental conditions), the rate of proton transport in UCPs was in the range between ≲5 and 30 μmol min^{-1} (mg of protein)$^{-1}$. As one can see in Table S3 of the Supporting Information, the reported values are variable and dependent on the experimental conditions. It is also worth mentioning that in many of the previous studies of proton transport by

dx.doi.org/10.1021/bi3003378 | *Biochemistry* 2012, 51, 4004−4014

reconstituted UCPs (Table S3 of the Supporting Information), the proton flux was dependent on the type and concentration of the fatty acid stimulant. The concentrations of the fatty acid required to reach the highest transport rate in these studies were typically higher than 100 μM, which was the concentration used in this study.

UCP-Mediated Chloride Transport. Anion transport has been previously shown for UCP1−UCP3.[34−36] In addition, the ability to form chloride channels has been reported for UCP1 and the second transmembrane helix (TM2) of UCP2.[37,38] In the study presented here, chloride ion transport of neuronal UCPs has been unambiguously detected. In L-α-lecithin vesicles, chloride ion influx (triggered by val) was observed for UCP2 and UCP4, but was very weak for UCP5 (Figure 3A−C). In comparison with that of the control protein-free vesicles, the fluorescence signal of the trapped fluorescent dye SPQ in UCP2 and UCP4 assays decreased drastically (an indication of the influx of chloride and anionic quenching of the trapped dye). In contrast, UCP5 proteoliposomes did not exhibit a significant reduction in the magnitude of the fluorescence signal. Similar to the proton transport case, introducing CL into the lipid system induced changes in the UCP-mediated chloride transport rate (Figure 3D,E). Compared to that in the lecithin vesicles, chloride transport flux in the CL/lecithin lipid system increased in both UCP2 and UCP5 (Figure 3E). This increase was significant for UCP5. Conversely, the rate of chloride transport by UCP4 was reduced by introduction of CL (Figure 3E). Thus, CL influences chloride transport of UCPs in a manner similar to that in the proton transport case. This observation could be important in understanding the mechanism of ion transport in UCPs. Overall, the chloride transport flux mediated by all neuronal UCPs was much lower compared to their proton transport rate.

Inhibition of UCP-Mediated Proton Flux by Purine Nucleotides. Besides being activated by fatty acids, the ion transport activity of UCPs is inhibited by purine nucleotides (ATP, ADP, GTP, and GDP).[1,2,4] In our previous conformational study, it was shown that all UCPs (UCP1−UCP5) interacted with purine nucleotides, resulting in minor conformational changes.[24] In this work, the presence of purine nucleotides resulted in a decrease in the rate of, but not full inhibition of, UCP-mediated proton transport in L-α-lecithin liposomes (Figure 4). It is worth mentioning that, under our experimental conditions, the maximal proton transport inhibition of UCPs was in the presence of 500 μM ATP. At this ATP level, compared to the original uninhibited flux, the proton transport rates of UCP2, UCP4, and UCP5 were decreased to 52, 67, and 63%, respectively (Figure 4A−C). Partial inhibition of proton transport of UCP1−UCP3 in the presence of a purine nucleotide was also observed in several previous studies (ref 5 and other references in Table S3 of the Supporting Information). This partial inhibition could be related to the physiological nature of purine nucleotide inhibition of proton transport in UCPs and/or the folded conformation of the reconstituted UCPs in liposomes. The extent of proton transport inhibition by ADP and ATP (500 μM) was different in each protein. For UCP2, ATP inhibited the proton transport more strongly than ADP (Figure 4A). This result is in agreement with a previous report by Echtay et al.[6] On the other hand, both ATP and ADP exhibited similar inhibitory effects on UCP4-mediated proton transport (Figure 4B). Finally, inhibition of UCP5-mediated proton transport by

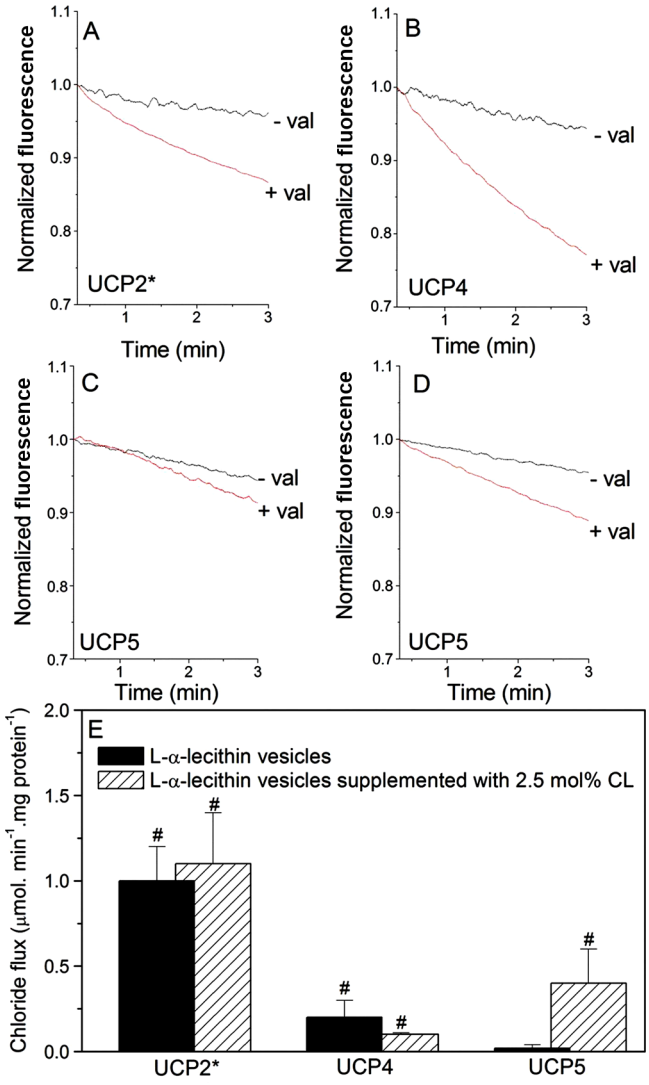

Figure 3. Transport of chloride mediated by neuronal UCPs across phospholipid vesicles. Direct SPQ fluorescence quenching measurement of chloride transport mediated by (A) UCP2*, (B) UCP4, (C) UCP5 in L-α-lecithin vesicles, and (D) UCP5 in L-α-lecithin vesicles with 2.5 mol % CL. Data were normalized to the initial fluorescence value. Chloride transport was initiated with 2 μM val. (E) Average corrected chloride transport rates mediated by neuronal UCPs in the two phospholipid systems. The transport rates were obtained in a manner similar to that used in proton transport experiments. The rates are the means of 15 independent measurements ± the standard error of the mean. In L-α-lecithin vesicles, chloride transport rates of UCP2*, UCP4, and UCP5 were 1.0 ± 0.2, 0.2 ± 0.01, and 0.02 ± 0.02 μmol min^{-1} (mg of protein)$^{-1}$, respectively. In L-α-lecithin vesicles with 2.5 mol % CL, these rates were 1.1 ± 0.3, 0.1 ± 0.01, and 0.4 ± 0.2 μmol min^{-1} (mg of protein)$^{-1}$, respectively. The phospholipid concentration was 20 mg/mL; the final protein content in the liposomes was 2−5 μg/mg of lipid. The final chloride transport rates were calculated on the basis of the total protein concentration in liposomes; the orientation of the reconstituted proteins were ignored in this calculation. A one-way ANOVA statistical test was performed to determine the statistical significance of data, and p values were obtained. $p < 0.05$ when comparing the chloride transport mediated by UCPs to the basal chloride leakage (#).

ADP was stronger than that of ATP (Figure 4C). These data indicate that purine nucleotides interact with all neuronal UCPs and inhibit their proton transport activity, albeit to different

dx.doi.org/10.1021/bi3003378 | Biochemistry 2012, 51, 4004−4014

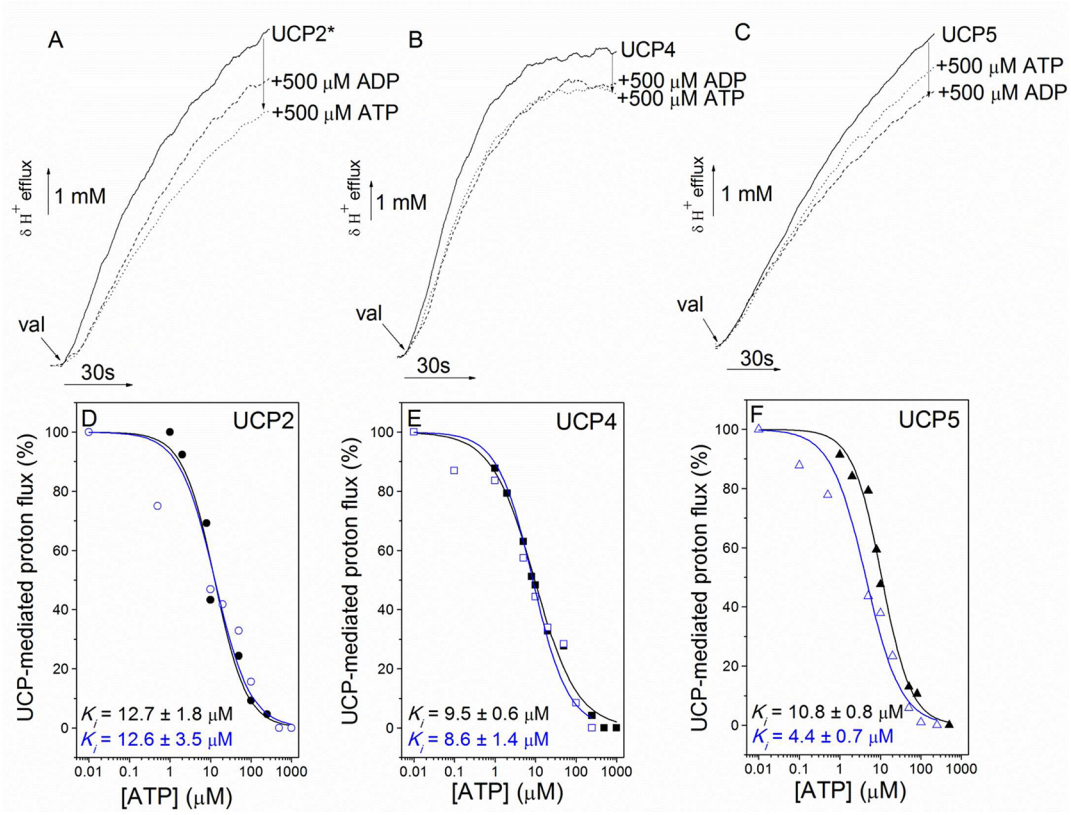

Figure 4. Inhibitory effect of purine nucleotides (ADP and ATP) on proton transport mediated by neuronal UCPs. Recorded H^+ efflux through L-α-lecithin vesicles reconstituted with (A) UCP2*, (B) UCP4, and (C) UCP5 in the presence and absence of 500 μM ATP or ADP. The purine nucleotides were incubated for 2 min with proteoliposomes prior to activation by LA and initiation (by 1 μM val) of proton flux. The inhibitory effects of ATP on UCP-mediated proton flux were measured and analyzed using the Hill equation (no cooperativity, Hill coefficient of 1). The K_i was estimated for binding affinity between ATP and (D) UCP2*, (E) UCP4, and (F) UCP5 reconstituted in L-α-lecithin vesicles. Empty and filled symbols represent the data points measured in the presence and absence of 2.5 mol % CL, respectively. The phospholipid concentration was 20 mg/mL; the final protein content in the liposomes was 2−5 μg/mg of lipid. The final proton transport rates were calculated in the presence of 100 μM LA and on the basis of the total protein concentration present in the liposomes; the orientations of the reconstituted proteins were ignored in this calculation.

extents. ATP inhibition of proton flux for neuronal UCPs was further quantified by concentration-dependent inhibition measurements to determine their relative affinity for the inhibitor. The inhibition constant (K_i) was determined for each protein and is shown in Figure 4D−F. The ATP inhibition constants were between 9 and 13 μM. These values are in the range of previously reported constants.[5,6] Addition of CL to the phospholipid vesicles did not create any significant changes in the ATP binding affinity for UCP2 and UCP4 (K_i values of 12.6 and 8.6 μM, respectively) (Figure 4). In contrast, UCP5 appeared to bind more strongly to ATP (K_i = 4.4 μM) in the presence of CL (Figure 4). To examine the orientation of UCPs after reconstitution into liposomes, we examined the inhibitory effect of ATP on proton transport with ATP on either or both sides of the liposome membranes. Comparison of the inhibition by external ATP or the combination of internal and external ATP suggests that UCP2 was reconstituted in the liposomes with no preference for one orientation or the other (Figure 5). This observation could partially explain the incomplete H^+ transport inhibition by ATP (see above). It is worth mentioning that the proton transport rate reported in this study was calculated for the total content of proteins in liposome.

Conformations of UCPs in Liposomes. Conformations of reconstituted UCPs in LUVs were measured using CD

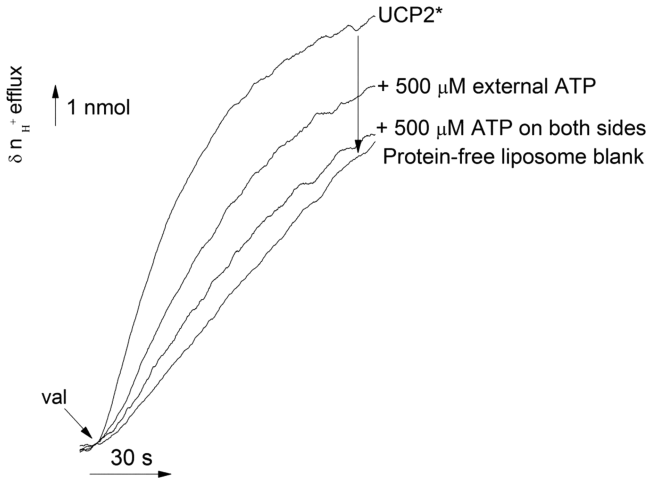

Figure 5. Orientation of reconstituted UCP2* (non-His-tagged UCP2) demonstrated through ATP inhibition. Recorded UCP2-mediated proton flux was partially inhibited by 500 μM external ATP and completely inhibited in the presence of 500 μM ATP on both sides of the bilayer. Proton transport by UCP2* was activated by 100 μM LA and initiated by addition of 1 μM val. All fluxes were corrected for and expressed as moles of H^+ efflux. Nonspecific proton leak is shown for protein-free liposomes.

dx.doi.org/10.1021/bi3003378 | *Biochemistry* 2012, 51, 4004−4014

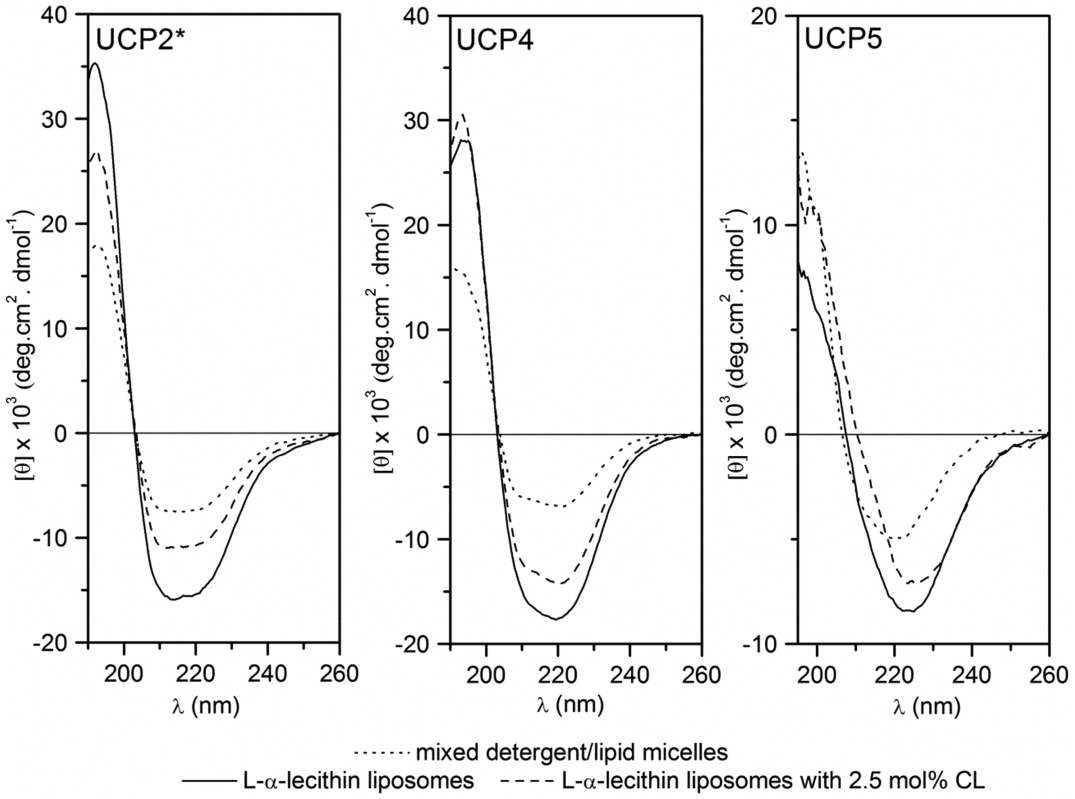

Figure 6. Comparative far-UV CD spectra of neuronal UCPs. Far-UV CD spectra of 2 μM UCPs in mixed detergent/lipid micelles (before reconstitution) are compared with the profiles of reconstituted UCPs in L-α-lecithin vesicles with and without 2.5 mol % CL. Protein and lipid concentrations were ~1 μM and 1 mM, respectively. All samples were measured in 10 mM potassium phosphate buffer (pH 7.2).

spectroscopy. Given CD signal detection limitations due to low signal-to-noise ratios at low protein concentrations (the minimal detectable protein concentration is typically between 0.5 and 1 μM), the protein:lipid molar ratio used for CD spectroscopic measurements was kept as low as 1:1000 (compared to 1:10000 in ion transport assays), where the protein concentration in liposomes was maintained at ~1 μM.

Refolding of UCPs was observed for all UCPs after reconstitution into liposomes (Figure 6). Compared with the mixed detergent/lipid micelle system (prior to reconstitution), UCP2 and UCP4 showed an enhancement in ellipticity after reconstitution into LUVs. In addition to increased ellipticity, the CD spectrum of UCP5 exhibited a red shift of the negative maximum (~220 nm) after reconstitution. Interestingly, each neuronal UCP took on a distinct conformation in liposomes. CD spectra of UCP2 and UCP4 indicate high α-helical contents for these proteins. The CD spectra of UCP2 contained two negative maxima (at ~220 and ~210 nm) and a positive maximum at ~192 nm (Figure 6). Spectra of UCP4 displayed one negative maximum at ~220 nm, a negative shoulder at ~210 nm, and a positive maximum at ~194 nm. CD spectra of both proteins exhibited typical helical conformations with the positive maximum:negative maximum ratio being ~2:1. The deconvolution of CD spectra revealed estimated helical contents of UCP2 and UCP4 in L-α-lecithin vesicles to be 53 and 52%, respectively (Table S2 of the Supporting Information). While displaying a transport activity comparative to those of the other two neuronal UCPs, at low protein:lipid ratios, UCP5 spectra showed a distinctly low helical content, with a negative maximum at ~220 nm and a positive maximum at ~192 nm (Figure 6).

In the presence of CL in liposomes, a decrease in negative ellipticity was consistently observed in all UCPs' CD spectra (Figure 6). CD spectra of UCPs in CL-supplemented vesicles maintained a shape and the location of maxima and minima similar to those in L-α-lecithin vesicles. The deconvolution of CD spectra in CL-supplemented vesicles also showed a decrease in the helical contents of all UCPs (Table S2 of the Supporting Information). This decrease in helical content can be indicative of CL-induced protein−protein interactions.[39] Changes in the helix packing and overall tertiary structure of UCPs in the presence of CL could also attribute to the decrease in helicity of the reconstituted proteins. Previous studies have demonstrated the importance of CL in possible dimerization or oligomerization of several mitochondrial proteins, such as AAC and ATP synthase.[18,40] Finally, addition of 100 μM ATP to both phospholipid systems resulted in negligible changes in the overall conformations of UCPs (Figure S2 of the Supporting Information). These observations were comparable to our previous conformational analysis of UCPs in a different lipid system.[24] As commonly observed, CD spectra of proteins reconstituted in liposome systems could be distorted because of flattening effects caused by light scattering.[39] This artifact could be the cause for lower positive ellipticities of the CD spectra of UCPs, especially UCP5 (Figure 6).

In our previous study,[24] UCP5 exhibited a higher helical content in detergents and other lipid systems than in the study presented here. It is plausible that in the lipid systems of this study, higher protein:lipid molar ratios promote protein association. To further explore the effect of the protein:lipid molar ratio on the size of the UCP5 proteoliposomes, the size of UCP5 proteoliposomes was estimated at different

dx.doi.org/10.1021/bi3003378 | *Biochemistry* 2012, 51, 4004−4014

protein:lipid ratios by DLS measurements (Figure S3 of the Supporting Information). The proteoliposome size varied inversely with protein:lipid molar ratio. As the protein:lipid ratio reached lower values, the size of the proteoliposome increased and was almost comparable to that of the blank liposomes, which implies that UCP5 can adopt a different and less associated (or more monomeric) conformation (Figure S3 of the Supporting Information). Attempts to further resolve the secondary structure of UCP5 using detergent SDS were also made. Increasing concentrations of SDS promoted the formation of monomers by disrupting the associated forms of UCP5, thus revealing its inherent secondary helical structures that could otherwise remain masked (Figure S4 of the Supporting Information).

DISCUSSION

This comparative study provides new experimental evidence of proton and chloride transport in neuronal uncoupling proteins, specifically UCP4 and UCP5, for which ion transport activity has not been reported previously. In addition, this study shows that CL influences both the conformational and ion transport properties of neuronal UCPs. These findings are essential in the search for the physiological roles of UCPs in the CNS and their uncoupling mechanism in the mitochondria.

UCP4 and UCP5 Exhibit UCP1-like Biophysical Properties. As mentioned previously, a low level of amino acid sequence identity to UCP1 and a lack of experimental evidence for direct ion transport activity have cast doubts on the physiological roles of UCP4 and UCP5.[1,2] Under our experimental conditions, these proteins mediate proton flux across phospholipid membranes in the presence of fatty acid activators (Figure 2). The proton transport is inhibited by purine nucleotides (Figure 4A−C), and the inhibition constants (K_i) for ATP are comparable for all three neuronal UCPs (Figure 4D−F). Multiple-sequence alignment of UCP4 and UCP5 with other UCPs in the family further confirms the experimental findings in this study.[24] Our previous sequence analysis showed that UCP4 and UCP5 conserved the negatively charged residues E34 (UCP4) and E55 (UCP5) located in TM-1 that are believed to be involved in proton binding of UCPs.[24,34] In addition, both UCP4 and UCP5 conserved three Arg residues in the even-numbered helices (TM-2, -4, and -6) that were proposed to be essential in nucleotide binding.[1,24] Thus, like other UCPs, UCP4 and UCP5 also exhibit nucleotide-sensitive proton transport across membranes.

Despite general structural (ref 24 and Figure 6) and functional similarity, the proton transport properties of neuronal UCPs are distinct from each other (Figures 2−4). Different uncoupling activities of neuronal UCPs were also observed in cell culture studies.[16,17] In this study, UCP2 and UCP5 displayed higher proton transport rates than UCP4, which were further enhanced by CL (Figure 2). On the other hand, UCP4 showed a lower transport rate, which did not vary significantly in the absence or presence of CL (Figure 2). The similar trend also applies to UCP-mediated chloride transport (Figure 3). Consequently, we conclude that both UCP4 and UCP5 show structural and functional characteristics comparable to those of other UCPs. These functions are, however, differentially modulated by purine nucleotides and lipid composition. In addition, each UCP, with a unique amino acid sequence, adopts a distinct conformation in the liposomes (Figure 6). Therefore, it is plausible that, in addition to sharing some common structural and functional features with other members of the UCP family, each neuronal UCP takes on a specific physiological role in the CNS.

The potential neuroprotective roles of neuronal UCPs have been the focus of recent studies.[2,4] The recent development of a UCP4-specific antibody has revealed UCP4 protein expression in the brain, with the highest protein content found in the cortex.[41] Finding UCP4 expression at the early embryonic stage that coincides with the beginning of neuronal differentiation could suggest a role for UCP4 in neuronal development and differentiation.[41] Given the lower ion transport activity of UCP4, it can be suggested that this protein may require activators other than (or in addition to) fatty acids for its effective proton transport function. As described by Sauer et al., ROS (at low concentrations) could act as a signaling mediator during cell growth and development.[42] Therefore, it is plausible that ROS may participate in the regulation of the UCP4 proton transport activity. So far, only UCP5 mRNA has been detected in brain tissues. Nevertheless, UCP5 mRNA transfected cells showed uncoupling activity and neuroprotective functions against oxidative stress.[14,17] Given the wider tissue distribution of UCP2 and UCP5 compared to that of UCP4 (almost exclusively in the brain), it is plausible that UCP4 participates in neuroprotection during early neuronal development, while UCP2 and UCP5 provide this protective function against oxidative stress in developed neurons and other tissues.

In addition to proton transport, all three neuronal UCPs also exhibited chloride transport activity (Figure 3). Evidence of chloride and anion transport by UCP1−UCP3 was also reported in previous studies.[34−38] A mutagenesis study of UCP1 identified that two intrahelical Arg residues (R83 and R91, located in TM-2) that are important for Cl^- transport.[43] Sequence alignment analysis showed that these two Arg residues were conserved in all five UCPs (except for UCP5 with the second Arg replaced with Lys).[24] Therefore, it is highly possible that these two Arg (Arg and Lys in UCP5) residues can also play a pivotal role in Cl^- transport in UCP2−UCP5. In fact, our ion transport study of the transmembrane segments of UCP2 highlighted the importance of these Arg residues in the chloride channel activity of TM2 in lipid bilayers.[38] Interestingly, R83 is one of the three conserved Arg residues involved in purine nucleotide binding, which inhibits proton and chloride transport mediated by UCPs.[1] Therefore, this conserved arginine, as a common site for anion transport and purine nucleotide substrate binding, can be significant in the regulation of chloride transport in UCPs.

Cardiolipin Influences the Structure and Function of Neuronal UCPs. It has been suggested that CL can play a crucial role in overall mitochondrial inner membrane organization and dynamics.[18,20−23,44,45] Mitochondrial carriers, including AAC, the phosphate carrier, and the carnitine/acylcarnitine transporter, all require CL for their transport activity in reconstituted systems.[46−48] To the best of our knowledge, the role of CL in the structure and function of neuronal UCPs has not been investigated in much detail. In this study, we showed that CL induced changes in proton and chloride transport activity by neuronal UCPs (Figures 2 and 3). Furthermore, reconstituted UCPs in CL-supplemented phospholipid vesicles could associate and/or enhance their intramolecular helix packing (Figure 6). These findings imply that CL can influence the structure, function, and physiological roles of UCPs in vivo. Given the high pI (~10) of all UCPs and the negative charge present in CL at physiological pH, it can be assumed that these molecules are electrostatically attracted to

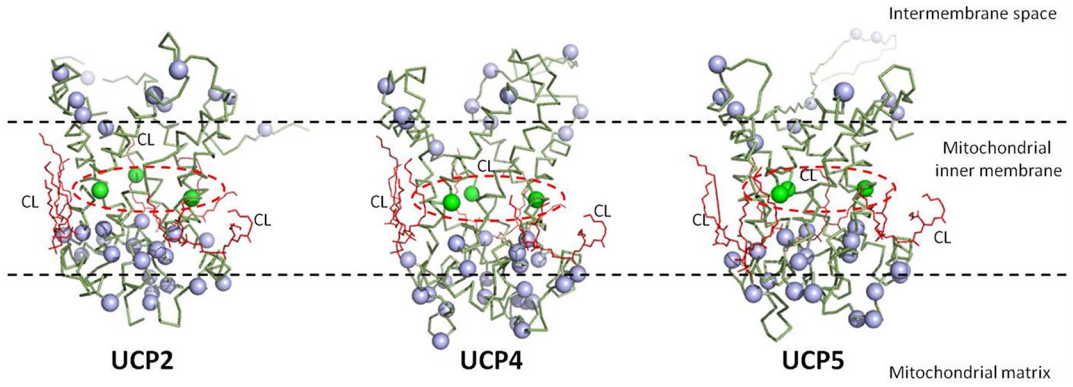

Figure 7. Hypothetical models of neuronal human UCPs. The models of UCPs were built on the basis of sequence alignment (T-Coffee) with the crystal structure of AAC bound to three CL molecules (Protein Data Bank entry 2C3E)[18] (see Experimental Procedures). The levels of sequence identity of UCP2, UCP4, and UCP5 compared to AAC are 24, 23, and 28%, respectively. Three conserved Arg residues (green spheres) participating in purine nucleotide binding[1,24] are located in the middle of the funnel-shaped UCP models. Basic amino acid residues (blue spheres) are mostly clustered in the cavity close to the matrix loops. Three CL molecules (in red), observed together with the AAC crystal structure, were superimposed onto the UCP models for analysis.[18] Interactions with CL can alter the structure and function of UCPs, as observed in the experimental data in this study.

each other. In fact, the crystal structure of AAC (also positively charged) exhibited a tightly bound 3CL–AAC complex.[18]

Among the neuronal UCPs, UCP4 seemed to be affected the least by CL. The overall charge of UCP4 is +6, compared to +12 in UCP5, +15 in UCP2, and +19 in AAC, which could result in a weaker interaction with CL in the reconstituted phospholipid system. As previously reported, the protein:CL molar ratio and the nature of the acyl hydrocarbon chains of CL could affect the structural and functional properties of anion carriers such as AAC.[23,45] UCP4's anomalous behavior in the presence of CL can also be attributed to these factors.

Ion Transport Mechanism of UCPs. It is important to note that FA-activated proton transport and substrate binding of UCPs are still poorly understood. Currently, there are two main hypotheses about the mechanism of proton transport by UCPs.[1] In the flip-flop model, protonated FA can flip-flop through the membrane bilayer and dissociate a proton in the matrix because of the difference in pH, and FA anions can be transported back by UCPs through an unknown mechanism.[1,5,36] The cofactor model, on the other hand, proposes that FA carboxyl groups can buffer protons, thus enhancing the rate of proton movement.[1,34,35] As the only high-resolution crystal structure available for the mitochondrial carrier family, the AAC structure has been used as a guideline to study the conformational and functional properties of other members of this family, including UCPs.[1,2,4] Despite sharing only 23% sequence identity, the recently reported NMR structure of UCP2 revealed a striking similarity with the AAC crystal structure.[3] On this basis, it can be suggested that other members of the mitochondrial carrier family could share the general structure features of AAC. In this study, three-dimensional structural models of three neuronal UCPs were generated on the basis of their sequence alignment with the AAC crystal structure (Figure 7 and Figure S5 of the Supporting Information). In all neuronal UCP models, the three conserved Arg residues (located on TM-2, -4, and -6) involved in nucleotide binding of UCPs[49] are located in the middle of the funnel-shaped structures, dividing the protein into two regions, cytoplasmic and matrix sides (Figure 7). This water-accessible cavity can be a potential active site for substrate binding and translocation.

A recent molecular modeling showed two conserved symmetric salt bridge networks in the intermembrane space ([FY][DE]XX[RK]) and matrix (PX[DE]XX[RK]) that could be important in substrate transport in mitochondrial carriers, including UCPs.[50] The authors also proposed the opening and closing of the carrier, coupled to the disruption and formation of the two salt bridge networks through a three-fold rotary twist could induce substrate binding and transport.[50] An analysis of the molecular models of the neuronal UCPs reveals an accumulation of positively charged residues at the bottom of the funnel-like structure close to the matrix, which is apparently accessible to both the matrix side and interior of the funnel (Figure 7). From the cytoplasmic side, this funnel-like domain is accessible to water molecules, and small anions such as chloride could potentially accumulate in the vicinity of the positively charged zone close to the bottom of the funnel through electrostatic interactions. The presence of a positively charged zone close to matrix, with the possibility of accessing both sides of the membrane, can generate a potential-sensitive charged area. The transmembrane energy barrier would therefore be reduced at the protein–matrix interface, and accumulation of small anions could result in lowering the membrane potential at this interface and inducing local conformational changes in the protein. This lowering of interface membrane potential can cause a channel-like opening resulting in anion flux across the membrane. Additionally, the existence of common amino acids in the purine nucleotide binding site and the anion transport pathway in UCPs implies that ion transport can be regulated by purine nucleotide binding. Evidence of ion channel properties of UCP1 and UCP2 was presented in previous studies.[37,38] In addition, the NMR structure of UCP2 exhibited a channel-like structure with openings on both sides.[3] Thus, on the basis of the experimental evidence provided by this and other studies for both carrier and channel-like mechanisms of ion transport in UCPs, it would be worthwhile to further explore a hypothetical coexistence of interconvertible carrier and channel modes as a mechanism for ion transport in UCPs.

There has been ample evidence showing that CL plays an important role in the structure and function of mitochondrial carriers, including UCPs[18,44–48] (Figures 2, 3, and 6). Some

studies speculated that this specific mitochondrial lipid could act as a mediator of associations between monomers.[18,51] Others provided evidence that mitochondrial carriers function as monomers.[52,53] In the UCP models generated here, three molecules of CL were observed to interact (through hydrophobic, electrostatic, and H-bond interactions) with amino acid residues that are situated toward the inner leaflet of the membrane and partially nested in small grooves formed by the matrix loops (Figure 7). These residues are located near the matrix salt bridge network that could be involved in transport activity of UCPs. Perhaps, if not participating in monomer association of carriers, CL might play a role in stabilizing this salt bridge network, which can act as a sensor in ion transport of UCPs and other mitochondrial carriers.

■ ASSOCIATED CONTENT

Supporting Information

Detailed UCP liposomal size, CD deconvolution results, and comparative proton transport of UCPs in previous studies (tables) and fluorescence spectroscopic monitoring of the removal of detergent from proteoliposomes, effects of ATP on far-UV CD spectra of reconstituted UCPs, UCP5 proteoliposome size, secondary structure of UCP5 in SDS, and overlap of three-dimensional structural UCP models. This material is available free of charge via the Internet at http://pubs.acs.org.

■ AUTHOR INFORMATION

Corresponding Author

*Department of Chemistry, Wilfrid Laurier University, 75 University Ave. W., Waterloo, ON N2L 3C5, Canada. Telephone: (519) 884-0710, ext. 2284. Fax: (519) 746-0677. E-mail: mjelokhani@wlu.ca.

Funding

This research was supported by grants from the Canada Foundation for Innovation (CFI) and the Natural Sciences and Engineering Research Council of Canada (NSERC) to M.J.-N. (CFI, 6786; NSERC, 250119) and M.D.S. (CFI, 11292; NSERC, 312143). T.H. has been the recipient of NSERC CGS Master's and Doctoral scholarships.

Notes

The authors declare no competing financial interest.

■ ACKNOWLEDGMENTS

We thank Marina Ivanova for technical support and for reading the manuscript.

■ ABBREVIATIONS

AAC, ADP/ATP carrier; BMCP, brain mitochondrial carrier protein; CAPS, 3-(cyclohexylamino)-1-propanesulfonic acid; CL, cardiolipin; CNS, central nervous system; C_8E_4, octyltetraoxyethylene; DLS, dynamic light scattering; DTT, dithiothreitol; FA, fatty acids; IPTG, isopropyl β-thiogalactopyranoside; LA, lauric acid; LUV, large unilamellar vesicle; NMR, nuclear magnetic resonance; PMSF, phenylmethanesulfonyl fluoride; ROS, reactive oxygen species; SDS, sodium dodecyl sulfate; SPQ, 6-methoxy-*N*-(3-sulfopropyl)quinolinium; TEA, tetraethylammonium; TES, *N*-[tris(hydroxymethyl)methyl]-2-aminoethanesulfonic acid; TM, transmembrane domain; TX, Triton X; UCP, uncoupling protein.

■ REFERENCES

(1) Krauss, S., Zhang, C. Y., and Lowell, B. B. (2005) The mitochondrial uncoupling protein homologs. *Nat. Rev. Mol. Cell Biol. 6*, 248−261.

(2) Echtay, K. S. (2007) Mitochondrial uncoupling proteins: What is their physiological role? *Free Radical Biol. Med. 43*, 1351−1371.

(3) Berardi, M. J., Shih, W. M., Harrison, S. C., and Chou, J. J. (2011) Mitochondrial uncoupling protein 2 structure determined by NMR molecular fragment searching. *Nature 476*, 109−113.

(4) Andrews, Z. B., Diano, S., and Horvath, T. L. (2005) Mitochondrial uncoupling proteins in the CNS: In support of function and survival. *Nat. Rev. Neurosci. 6*, 829−840.

(5) Jaburek, M., and Garlid, K. D. (2003) Reconstitution of recombinant uncoupling proteins: UCP1, -2, and -3 have similar affinities for ATP and are unaffected by coenzyme Q_{10}. *J. Biol. Chem. 278*, 25825−25831.

(6) Echtay, K. S., Winkler, E., Frischmuth, K., and Klingenberg, M. (2001) Uncoupling proteins 2 and 3 are highly active H^+ transporters and highly nucleotide sensitive when activated by coenzyme Q (ubiquinone). *Proc. Natl. Acad. Sci. U.S.A. 98*, 1416−1421.

(7) Jezek, P., and Urbankova, E. (2000) Specific sequence motifs of mitochondrial uncoupling proteins. *IUBMB Life 49*, 63−70.

(8) Mao, W., Yu, X. X., Zhong, A., Li, W., Brush, J., Sherwood, S. W., Adams, S. H., and Pan, G. (1999) UCP4, a novel brain-specific mitochondrial protein that reduces membrane potential in mammalian cells. *FEBS Lett. 443*, 326−330.

(9) Zhang, M., Wang, B., Ni, N. Y. H., Liu, F., Fei, L., Pan, X. Q., Guo, M., Chen, R. H., and Guo, X. R. (2006) Overexpression of uncoupling protein 4 promotes proliferation and inhibits apoptosis and differentiation of preadipocytes. *Life Sci. 79*, 1428−1435.

(10) Sanchis, D., Fleury, C., Chomiki, N., Goubern, M., Huang, Q., Neverova, M., Gregoire, F., Easlick, J., Raimbault, S., Levi-Meyrueis, C., Miroux, B., Collins, S., Seldin, M., Richard, D., Warden, C., Bouillaud, F., and Ricquier, D. (1998) BMCP1, a novel mitochondrial carrier with high expression in the central nervous system of humans and rodents, and respiration uncoupling activity in recombinant yeast. *J. Biol. Chem. 273*, 34611−34615.

(11) Fridell, Y. W. C., Sanchez-Blanco, A., Silvia, B. A., and Helfand, S. L. (2004) Functional characterization of a *Drosophila* mitochondrial uncoupling protein. *J. Bioenerg. Biomembr. 36*, 219−228.

(12) Yu, X. X., Mao, W., Zhong, A., Schow, P., Brush, J., Sherwood, S. W., Adams, S. H., and Pan, G. (2000) Characterization of novel UCP5/BMCP1 isoforms and differential regulation of UCP4 and UCP5 expression through dietary or temperature manipulation. *FASEB J. 14*, 1611−1618.

(13) Ledesma, A., Lacoba, M. G., and Rial, E. (2002) The mitochondrial uncoupling proteins. *Genome Biol. 3*, 3015.1−3015.9.

(14) Kim-Han, J. S., Reichert, S. A., Quick, K. L., and Dugan, L. L. (2001) BMCP1: A mitochondrial uncoupling protein in neurons which regulates mitochondrial function and oxidant production. *J. Neurochem. 79*, 658−668.

(15) Mattson, M. P., and Liu, D. (2003) Mitochondrial potassium channels and uncoupling proteins in synaptic plasticity and neuronal cell death. *Biochem. Biophys. Res. Commun. 304*, 539−549.

(16) Chu, A. C., Ho, P. W., Kwok, K. H., Ho, J. W., Chan, K. H., Liu, H. F., Kung, M. H., Ramsden, D. B., and Ho, S. L. (2009) Mitochondrial UCP4 attenuates MPP^+ and dopamine-induced oxidative stress, mitochondrial depolarization, and ATP deficiency in neurons, and is interlinked with UCP2 expression. *Free Radical Biol. Med. 46*, 810−820.

(17) Kwok, K. H., Ho, P. W., Chu, A. C., Ho, J. W., Liu, H. F., Yiu, D. C., Chan, K. H., Kung, M. H., Ramsden, D. B., and Ho, S. L. (2010) Mitochondrial UCP5 is neuroprotective by preserving mitochondrial membrane potential, ATP levels, and reducing oxidative stress in MPP^+ and dopamine toxicity. *Free Radical Biol. Med. 49*, 1023−1035.

(18) Nury, H., Dahout-Gonzalez, C., Trezeguet, V., Lauquin, G., Brandolin, G., and Pebay-Peyroula, E. (2005) Structural basis for lipid-mediated interactions between mitochondrial ADP/ATP carrier monomers. *FEBS Lett. 579*, 6031−6036.

(19) Kagan, V. E., Tyurin, V. A., Jiang, J., Tyurina, Y. Y., Ritov, V. B., Amoscato, A. A., Osipov, A. N., Belikova, N. A., Karpalov, A. A., Kini, V., Vlasova, I. I., Zhao, Q., Zou, M., Di, P., Svistunenko, D. A., Kurnikov, I. V., and Borisenko, G. G. (2005) Cytochrome c acts as a cardiolipin oxygenase required for release of proapoptotic factors. *Nat. Chem. Biol. 1*, 223−232.

(20) Eble, K. S., Coleman, W. B., Hantgan, R. R., and Cunningham, C. C. (1990) Tightly associated cardiolipin in the bovine heart mitochondrial ATP synthase as analyzed by ^{31}P nuclear magnetic resonance spectroscopy. *J. Biol. Chem. 265*, 19434−19440.

(21) Pfeiffer, K., Gohli, V., Stuart, R. A., Hunte, C., Brandt, U., Greenberg, M. L., and Schagger, H. (2003) Cardiolipin stabilizes respiratory chain supercomplexes. *J. Biol. Chem. 278*, 52873−52880.

(22) Haines, T. H. (2009) A new look at cardiolipin. *Biochim. Biophys. Acta 1788*, 1997−2002.

(23) Klingenberg, M. (2009) Cardiolipin and mitochondrial carriers. *Biochim. Biophys. Acta 1788*, 2048−2058.

(24) Ivanova, M. V., Hoang, T., McSorley, F. R., Krnac, G., Smith, M. D., and Jelokhani-Niaraki, M. (2010) A comparative study on conformation and ligand binding of the neuronal uncoupling proteins. *Biochemistry 49*, 512−521.

(25) Jelokhani-Niaraki, M., Ivanova, M. V., McIntyre, B. L., Newman, C. L., McSorley, F. R., Young, E. K., and Smith, M. D. (2008) A CD study of uncoupling protein-1 and its transmembrane and matrix-loop domains. *Biochem. J. 411*, 593−603.

(26) Lowry, O. H., Rosebrough, N. J., Farr, A. L., and Randall, R. J. (1951) Protein measurement with the folin phenol reagent. *J. Biol. Chem. 193*, 265−275.

(27) Whitmore, L., and Wallace, B. A. (2004) Dichroweb: An online server for protein secondary structure analyses from circular dichroism spectroscopic data. *Nucleic Acids Res. 32*, W668−W673.

(28) Lees, J. G., Miles, A. J., Wien, F., and Wallace, B. A. (2006) A reference database for circular dichroism spectroscopy covering fold and secondary structure space. *Bioinformatics 22*, 1955−1962.

(29) Orosz, D. E., and Garlid, K. D. (1993) A sensitive new fluorescence assay for measuring proton transport across liposomal membranes. *Anal. Biochem. 210*, 7−15.

(30) Poirot, O., O'Toole, E., and Notredame, C. (2003) Tcoffee@ igs: A web server for computing, evaluating and combining multiple sequence alignments. *Nucleic Acids Res. 31*, 3503−3506.

(31) Notredame, C., Higgins, D. G., and Heringa, J. (2000) T-Coffee: A novel method for fast and accurate multiple sequence alignment. *J. Mol. Biol. 302*, 205−217.

(32) Sali, A., Potteron, L., Yuan, F., Vlijimen, H. V., and Karplus, M. (1995) Evaluation of comparative protein folding by MODELLER. *Proteins 23*, 318−326.

(33) DeLano, W. L. (2002) *PyMOL*, DeLano Scientific, San Carlos, CA.

(34) Echtay, K. S., Winkler, E., Bienengraeber, M., and Klingenberg, M. (2000) Site-directed mutagenesis identifies residues in uncoupling protein (UCP1) involved in three different functions. *Biochemistry 39*, 3311−3317.

(35) Klingenberg, M., and Echtay, K. S. (2001) Uncoupling proteins: The issues from a biochemist point of view. *Biochim. Biophys. Acta 1504*, 128−143.

(36) Garlid, K. D., Orosz, D. E., Modriansky, M., Vassanelli, S., and Jezek, P. (1996) On the mechanism of fatty acid-induced proton transport by mitochondrial uncoupling protein. *J. Biol. Chem. 271*, 2615−2620.

(37) Huang, S. G., and Klingenberg, M. (1996) Chloride channel properties of the uncoupling protein from brown adipose tissue mitochondria: A patch-clamp study. *Biochemistry 35*, 16806−16814.

(38) Yamaguchi, H., Jelokhani-Niaraki, M., and Kodama, H. (2004) Second transmembrane domain of human uncoupling protein 2 is essential for its anion channel formation. *FEBS Lett. 577*, 299−304.

(39) Mao, D., and Wallace, B. A. (1984) Differential light scattering and absorption flattening optical effects are minimal in the circular dichroism spectra of small unilamellar vesicles. *Biochemistry 23*, 2667−2673.

(40) Acehan, D., Malhotra, A., Xu, Y., Ren, M., Stokes, D. L., and Schlame, M. (2011) Cardiolipin affects the supramolecular organization of ATP synthase in mitochondria. *Biophys. J. 100*, 2184−2192.

(41) Smorodchenko, A., Ruppercht, A., Sarilova, I., Ninnemann, O., Brauer, A. U., Franke, K., Schumacher, S., Techritz, S., Nitsch, R., Schuelke, M., and Pohl, E. E. (2009) Comparative analysis of uncoupling protein 4 distribution in various tissues under physiological conditions and during development. *Biochim. Biophys. Acta 1788*, 2309−2319.

(42) Sauer, H., Wartenberg, M., and Hescheler, J. (2001) Reactive oxygen species as intracellular messengers during cell growth and differentiation. *Cell. Physiol. Biochem. 11*, 173−186.

(43) Echtay, K. S., Bienengraeber, M., and Klingenberg, M. (2001) Role of intrahelical arginine residues in functional properties of uncoupling protein (UCP1). *Biochemistry 40*, 5243−5248.

(44) Mende, P., Kolbe, H. V., Kadenbach, B., Stipani, I., and Palmieri, F. (1982) Reconstitution of the isolated phosphate-transport system of pig-heart mitochondria. *Eur. J. Biochem. 128*, 91−95.

(45) Beyer, K., and Klingenberg, M. (1985) ADP/ATP carrier protein from beef heart mitochondria has high amounts of tightly bound cardiolipin, as revealed by ^{31}P nuclear magnetic resonance. *Biochemistry 24*, 3821−3826.

(46) Kadenbach, B., Mende, P., Kolbe, H. V., Stipani, I., and Palmieri, F. (1982) The mitochondrial phosphate carrier has essential requirement for cardiolipin. *FEBS Lett. 139*, 109−112.

(47) Hoffman, B., Stockl, A., Schlame, M., Beyer, K., and Klingenberg, M. (1994) The reconstituted ADP/ATP carrier activity has an absolute requirement for cardiolipin as shown in cysteine mutants. *J. Biol. Chem. 269*, 1940−1944.

(48) Noel, H., and Pande, S. V. (1986) An essential requirement of cardiolipin for mitochondrial carnitine acylcarnitine translocase activity. Lipid requirement of carnitine acylcarnitine translocase. *Eur. J. Biochem. 155*, 99−102.

(49) Modriansky, M., Murdza-Inglis, D. L., Patel, H. V., Freeman, K. B., and Garlid, K. D. (1997) Identification by site-directed mutagenesis of three arginines in uncoupling protein that are essential for nucleotide binding and inhibition. *J. Biol. Chem. 272*, 24759−24762.

(50) Robinson, A. J., Overy, C., and Kunji, E. R. S. (2008) The mechanism of transport by mitochondrial carriers based on analysis of symmetry. *Proc. Natl. Acad. Sci. U.S.A. 105*, 17766−17771.

(51) Nury, H., Dahout-Gonzalez, C., Trezeguet, V., Lauquin, G., Brandolin, G., and Pebay-Peyroula, E. (2006) Relations between structure and function of the mitochondrial ADP/ATP carrier. *Annu. Rev. Biochem. 75*, 713−741.

(52) Bamber, L., Harding, M., Monne, M., Slotboom, D.-J., and Kunji, E. R. S. (2007) The yeast mitochondrial ADP/ATP carrier functions as a monomer in mitochondrial membranes. *Proc. Natl. Acad. Sci. U.S.A. 104*, 10830−10834.

(53) Nury, H., Manon, F., Arnou, B., Maire, M., Pebay-Peyroula, E., and Ebel, C. (2008) Mitochondrial bovine ADP/ATP carrier in detergent is predominantly monomeric but also forms multimeric species. *Biochemistry 47*, 12319−12331.